Junoite, $Cu_2Pb_3Bi_8(S,Se)_{16}$, a New Sulfosalt from Tennant Creek, Australia: Its Crystal Structure and Relationship with Other Bismuth Sulfosalts

WILLIAM G. MUMME

CSIRO, Division of Mineral Chemistry, P.O. Box 124, Port Melbourne, Victoria 3207, Australia

Abstract

Junoite, $Cu_2Pb_3Bi_8(S,Se)_{16}$, (S:Se = 5:1), is monoclinic, space group $C2/m$ with $a = 26.66(1)$, $b = 4.06(1)$, $c = 17.03(1)$ Å and $\beta = 127.20(2)°$. Diffractometer data were recorded with an equi-inclination diffractometer equipped with a proportional counter; the structure was solved using the Patterson method. Least squares refinement reduced the R value to 11.0 percent and permitted distinction of Pb and Bi on the basis of bond distances. The asymmetric unit of the unit cell contains 2 Pb, 4 Bi, 1 Cu, and 8 S atoms. The lead atom at the origin has octahedral coordination, while the other lead atom has eight-fold coordination. Three of the bismuth atoms have three sulfur neighbors at distances ranging from 2.51 to 2.89 Å while there is evidence for selenium ordering in the structure which results in larger than average bonding distances in the fourth $Bi(S,Se)_3$ group. Copper has distorted tetrahedral coordination with bonds ranging from 2.32 to 2.52 Å in length.

A survey of dimensions of the BiS_3 anionic group in bismuth sulfosalts is also reported; average lengths of Bi–S non-bridge bonds and S–Bi–S bridge bonds were found to be 2.63 and 2.76 Å, respectively.

Junoite and other bismuth sulfosalts can be successfully classified on the basis of the dimensional relationship between the coordination polyhedra around the monovalent and divalent atoms, and the coordination polyhedra around the trivalent atoms (Takeuchi and Sadanaga's 1969 system of classification).

Introduction

Edwards (1955) identified bismuthinite, native bismuth, and matildite in the Peko copper ore body at Tennant Creek. He also found a fourth bismuth mineral, mostly intergrown with bismuthinite, which yielded positive microchemical tests for both lead and bismuth.

More recently the Juno ore body at Tennant Creek has been mined and treated by Peko-Wallsend Ltd. for gold, bismuth, copper, silver and selenium. The deposit is made up of smaller ore bodies which are usually zoned with an outer shell of dolomite, an inner shell of magnetic-dolomite rock, and a core of massive magnetite containing the ore minerals, and some silicates (Hamilton, 1970; also Large, 1974b).

Fander (1966), using electron probe techniques and ore microscopy, discovered the presence of selenium in drill intersections of the No. 1 ore body at Juno which he concluded was present as guanajuatite, $Bi_2(S,Se)_3$. Later electron probe analyses of bismuth minerals in the tailings from the Juno Mine ore, which were carried out by Hendley and Schultz (1972), showed that they contained lead, copper, and selenium (up to 24 percent). Many compositions determined by Hendley and Schultz did not fall on the bismuthinite-aikinite join; these indicated that there was not a definite substitution of (Cu + Pb) for Bi in all Juno "bismuthinite," as indicated previously by the work of Padera (1956) and Welin (1966). Hendley and Schultz proposed the existence of extensive solid solution of cations and anions between bismuthinite and aikinite.

Large (1974a) identified, and Large and Mumme (1975) isolated, from the Juno mine ore body specimens, seleniferous bismuth-lead-copper sulfosalts, one of which was found by electron probe microanalysis to have the average composition $Cu_{0.49}Pb_{0.73}Bi_2S_{3.12}Se_{0.73}$ (Table 1) and was named junoite. The composition of junoite is close to that of $CuPbBi_3S_6$ (krupkaite; Mumme, 1975), but it has a lead:copper ratio substantially greater than unity, which distinguishes it from any member of the

bismuthinite–aikinite series. The mineral rezbanyite, originally described by Johansson (1924a) as $Cu_2Pb_3Bi_{10}S_{19}$, also has a composition close to that of junoite, although more recent studies of rezbanyite by Padera (1956) and Welin (1966) have indicated that it has a composition of $CuPbBi_5S_9$ and is a member of the bismuthinite–aikinite series identical with gladite.

Seleniferous lead-bismuth sulfosalts have been reported from Falun, Sweden, where the material originally described by Weibull (1885) and Johansson (1924b)—given variously the names weibullite, seleniferous cheviatite, and seleniferous galenobismutite— was found by Peacock and Berry (1940) to be an intergrowth of two minerals later referred to as weibullite and selenjoseite (Berry and Thompson, 1962). Karup-Moller (1970) reinvestigated the original sample of weibullite from Falun, and gave chemical data and physical properties for the two phases. He found selenjoseite to be equivalent to laitakarite, $(Bi,(Pb))_4SSe_2$, and gave weibullite the composition $Bi_6Pb_4S_9Se_4$. Johansson (1924b) identified another seleniferous phase from Falun which he named wittite $(Bi_6Pb_5S_{11}Se_3)$. Ontoev, Troneva, and Tsepin (1972) have reported an argentiferous variety of wittite from the USSR.

Other seleniferous bismuth-lead sulfosalts reported include platynite, $Bi_7Pb_4S_4Se_7$, by Flink (1910) and Sindeeva (1962); selencosalite by Odman (1941); and seleniferous lillianite, $Pb_3Bi_2(S,Se)_6$, and selengoongarite, $Pb_4Bi_2(S,Se)_7$, by Isacsson (see Grip and Wirstam, 1970). The characteristic presence of selenium in the composition of these lead-bismuth sulfosalts is explained by taking into account the size of the bismuth atoms and their pronounced affinity towards selenium and tellurium. For example, platynite has been reported to contain up to 19.45 percent Se. Even so, of the above reported occurrences, only two species—namely, laitakarite and weibullite—have been well characterized, while the others are of doubtful status and deserve reinvestigation. Wittite in particular needs single crystal data to distinguish it from weibullite (Large and Mumme, 1975).

Because junoite, with up to 11.4 percent selenium, is one of a unique group of minerals, the knowledge of its crystal structure is important in relating it to other seleniferous varieties of lead-bismuth sulfosalts.

Experimental

Crystals of junoite were isolated from hand specimen R27790 (Large and Mumme, 1975). X-ray

TABLE 1. Microprobe Analyses of Junoite

	Previous Average*	R27790**	
		1	2
Bi	56.5	57.2	59.0
Pb	20.3	20.6	20.9
Cu	4.2	3.9	3.9
Ag	--	--	--
Fe	--	--	--
S	13.5	12.8	12.6
Se	7.8	7.6	5.6
Atomic proportions based on 8.00 Bi			
Bi	8.00	8.00	8.00
Pb	2.92	2.92	2.88
Cu	1.96	1.80	1.76
S	12.48	11.68	11.56
Se	2.92	2.80	2.00

*The average of nine analyses reported in Large and Mumme (1975).
**Analyses by D. Wark (Geology Department, University of Melbourne).

Weissenberg films were taken of these crystals and electron probe analyses were performed on two of several crystal fragments which gave identical X-ray data. These analyses by D. Wark, Melbourne University, gave the average composition $Cu_{0.45}Pb_{0.73}Bi_2S_{2.90}Se_{0.6}$ (Table 1) and verified that the correct mineral had been isolated. The precise unit cell parameters for junoite—$a = 26.66(1)$, $b = 4.06(1)$, $c = 17.03(1)$Å, $\beta = 127.20(2)°$, $\rho_{calc} = 6.77$ g cm^{-3}— were derived by refining X-ray powder diffractometer data (Table 2), indexed with the aid of the single crystal Weissenberg films. This powder data was recorded with $CuK\alpha$ monochromated radiation, using slow scans (1/4°/min) and KCl ($a_0 = 6.2929$ Å) as an internal standard.

The systematic absences on the $h0l$, $h1l$ and $h2l$ Weissenberg films recorded around the short 4Å axis—namely, hkl, $h + k \neq 2n + 1$; $h0l$, $h \neq 2n$— defined the space group alternatives as $C2/m$, Cm, or $C2$. It was assumed that the centrosymmetric space group $C2/m$ was the most probable, a choice which was later confirmed by the satisfactory solution and refinement of the structure.

Integrated intensities for the 683 independent reflections were measured with an ω-scan (*i.e.*, rotating crystal, stationary counter) performed with the aid of an automatic equi-inclination Stoe diffractometer equipped with a proportional counter as a detector.

Junoite has a very high linear absorption coefficient (1345 cm^{-1} for $CuK\alpha$) and it was difficult to obtain a suitable crystal for data collection, because small scale irregularities in the crystal shape, which would have had little effect in a material with a lower

TABLE 2. Refined X-ray Powder Data for Junoite (CuKα)

I	d(meas)	d(calc)	hkl	I	d(meas)	d(calc)	hkl
2	6.515	6.498	$40\bar{2}$	2	2.832	2.831	113
		6.434	$40\bar{1}$			2.832	$60\bar{6}$
2	5.433	5.416	$40\bar{3}$	1	2.796	2.796	312
½	4.595	4.589	202	1	2.712	2.711	005
1	4.084	4.077	$60\bar{1}$			2.709	$80\bar{6}$
½	4.005	4.005	$20\bar{4}$	2	2.606	2.605	$51\bar{5}$
8	3.904	3.942	$11\bar{1}$			2.620	$71\bar{1}$
		3.888	$60\bar{4}$			2.600	$10,0\bar{5}$
1	3.681	3.707	111	1	2.538	2.549	$31\bar{5}$
		3.683	$31\bar{1}$	2	2.506	2.502	$10,0\bar{2}$
1	3.590	3.593	$31\bar{2}$	1	2.462	2.456	$10,0\bar{6}$
10	3.545	3.516	310	2	2.384	2.380	914
		3.536	600			2.382	$91\bar{3}$
½	3.471	3.469	203	1½	2.320	2.317	$51\bar{6}$
4	3.388	3.388	004			2.313	$91\bar{2}$
		3.379	$40\bar{5}$			2.322	$10,0\bar{1}$
1	3.314	3.296	$31\bar{3}$			2.210	603
		3.334	$60\bar{5}$	4	2.213	2.218	$12,0\bar{5}$
		3.316	402			2.208	$12,0\bar{4}$
½		3.273	112	1	2.141	2.139	314
5	3.229	3.249	$80\bar{4}$	2	2.103	2.101	$60\bar{8}$
		3.216	$80\bar{2}$	3	2.095	2.092	513
3	3.175	3.179	311	4	2.070	2.068	$11\bar{6}$
		3.170	$11\bar{3}$			2.067	$10,0\bar{8}$
1	3.131	3.116	$20\bar{5}$			2.066	$11,1\bar{5}$
		3.125	$51\bar{3}$			2.078	$11,1\bar{4}$
		3.148	$51\bar{1}$			2.071	$12,0\bar{7}$
4	2.970	2.962	$80\bar{1}$	2	2.026	2.027	020
7	2.919	2.916	$31\bar{4}$	2	1.999	2.002	$22\bar{1}$
		2.930	510			1.999	712

distance, of 4.06 Å, which allows only the two-fold and four-fold sites at $y = 0$ and $y = \frac{1}{2}$ of the assumed space group $C2/m$ to be occupied, suggested that the unit cell contents were $Pb_6Cu_4Bi_{16}(S,Se)_{32}$, with S:Se approximately equal to 5:1, and that one lead atom occupied a two-fold site at the origin. The solution of the structure was therefore attempted using only the $h0l$ data, from which a Patterson function $P(u,0,w)$ was calculated. Structure factors and electron density calculations for a model derived from this Patterson projection located all the atoms on the (010) projection. Bond length considerations were helpful in assigning the y parameters of 0 or ½, and finally all positions were refined by least-squares refinement of the three dimensional intensity data using a version of ORFLS (Busing, Martin, and Levy, 1962) obtained from the University of Canterbury, New Zealand, for which the weighting scheme of Cruickshank *et al* (1961) was used.

Neutral-atom scattering curves were used (Cromer and Waber, 1965) and anomalous dispersion corrections were made for lead and bismuth. As the average Se content for the specimen is 6.6 percent, a scattering curve of f (0.15 Se + 0.85 S) was originally used for the non-metal atoms.

The final R value of 12.0 percent (see below) was somewhat high, possibly due to anisotropic vibration of the metal atoms, the effects of absorption, and errors in the assumed composition. Attempts were made to isolate other smaller crystals with even more equidimensional cross sections, but none were obtained, due mainly to the natural cleavage habit of the mineral. Further improvements in the R value may be expected with a sample ground to a sphere, but the cleavage habit, the small size of the crystals isolated, and the softness of the material will make the preparation of such a sample difficult.

absorption factor, limited the accuracy of absorption corrections. Most crystals isolated from the specimen were of highly irregular shapes, but one reasonably regular prismatic fragment (0.11 × 0.075 × 0.22 mm) was obtained from which a satisfactory data set was recorded. Background intensity was recorded for 100 sec at ± 2° from the intensity maximum together with the total number of counts accumulated as the crystal rotated through 4° in ϕ at a slow scanning rate 4°/200 sec. An absorption factor obtained by the empirical method attributed to North, Phillips, and Mathews by Arndt and Willis (1966) was applied to the data, and the integrated intensities were corrected for Lorentz and polarization effects using programs developed for an 803 Elliott computer by Daly, Stephens, and Wheatley (1963). Intensities were considered to be less than a detectable value when $BG + 0.67\sigma BG > P - 0.67\sigma BG$, where BG is the integrated background count, P the total number of counts accumulated, and 0.67σ the probable error computed from counting statistics (Arndt and Willis, 1966).

Structure Determination and Refinement

An ideal formula $Cu_{0.5}Pb_{0.75}Bi_2(S,Se)_4$ was deduced from the compositions determined by the electron probe analyses. This, together with the short b repeat

Description of the Structure

In the structure of junoite (Fig. 1) one lead and two bismuth atoms occupy the three octahedrally coordinated sites, while a further bismuth atom and a further lead atom respectively occupy 7- and 8- coordinated sites. The copper atoms all occupy equivalent tetrahedral sites which share edges with one another. Zig-zag ribbons of edge-shared octahedra, cross-linked by further pairs of edge-shared octahedra, provide a framework (Fig. 2) which is filled by the bismuth and lead atoms in 7- and 8-fold coordination, and by the pairs of tetrahedrally-coordinated copper atoms.

$M(2)$, $M(4)$, and $M(5)$ have nearest neighbor ap-

proaches of sulfur atoms at about 2.7 Å or less, in agreement with the more covalent character of the Bi–S bonds, while $M(3)$ has longer bond distance of 2.9 to 3.4 Å, in agreement with Pb–S distance in galena and other lead sulfosalts (Nowacki, 1969). $M(1)$ and $M(6)$ both have M–S distances which are not substantially different, so that although it would be expected that $M(6)$, the two-fold site, would be occupied by Pb and $M(1)$ by Bi, to yield the ideal composition $Pb_6Bi_{10}Cu_4(S,Se)_{32}$, there appears to be no distinction on the grounds of bond lengths for these two sites (see Table 4).

While the copper is approximately described as having tetrahedral coordination, it has in fact three neighbors located at 2.32 Å and one at a longer than average distance of 2.52 Å. The coordination is therefore intermediate between three-fold planar and tetrahedral. Thus in tetrahedrite (Wuensch, 1964) Cu–S_3 (planar) is 2.25 Å, and Cu–S_4 (tetrahedral) averages 2.35 Å (Berry, 1965). The distortion away from ideal tetrahedral coordination is evidenced by the bond angles which range from 100.2 to 122.2 as compared to 109.5 for a regular tetrahedron.

Final atomic positions and bond lengths and angles are given in Tables 3 and 4. The observed and calculated structure factors are listed in Table 5.

Ordering of Selenium

Refinement of the junoite structure, using an average scattering factor of f (0.15 Se + 0.85 S), yielded a final R value of 12.0 percent. The Fourier map indicated peak heights for S(3) and S(8) which were about 50 percent and 30 percent greater than the average height of the other six sulfur atoms (see Table 6); the values given in Table 6 show that the isotropic temperature factors for the sulfur atoms in
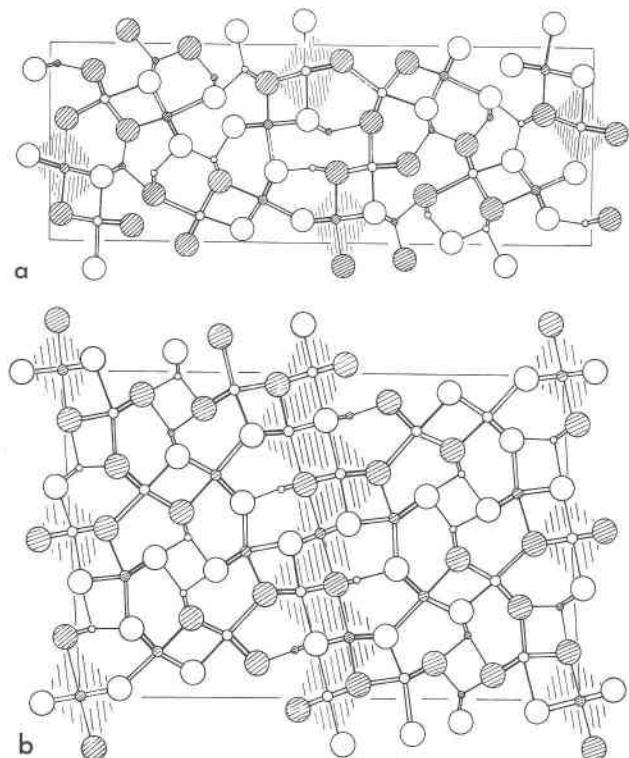

FIG. 2. Diagrams of the bismuth sulfosalt structures: (a) $Cu_4Bi_4S_9$; (b) hodrushite. Notation is the same as in Figure 1.

sites S(3) and S(8) were significantly lower than those for the other sites.

These observations suggested that the S(3) and S(8) sites contained more selenium than the other six. Calculations based on these assumptions gave a slightly lower R value of 11.0 percent and temperature factors for all the non-metal atom sites which were more consistent, when refinement was

FIG. 1. Junoite as an assemblage of octahedra and other coordination polyhedra. The shaded portions are equivalent to fragments of the PbS type. Hatched circles are at ½, open circles at 0. Small circles Cu; medium circles Pb, Bi; large circles S.

TABLE 3. Atomic Coordinates in Junoite

Site	Occupancy	x	y	z	$B(Å)^2$
M1	Bi	0.1486(3)	½	0.2326(4)	4.07(15)
M2	Bi	.3102(3)	0	.4799(4)	3.63(14)
M3	Pb	.0205(3)	0	.2772(5)	5.13(18)
M4	Bi	.3560(3)	0	.2682(5)	4.25(16)
M5	Bi	.3244(3)	½	.0249(4)	4.11(16)
M6	Pb	.0000	0	.0000	3.97(21)
S1	S	.1323(14)	0	.1044(22)	3.4(68)
S2	S	.1557(13)	0	.3653(20)	3.1(62)
S3	(.75Se + .25S)	.2870(9)	½	.3451(14)	3.0(41)
S4	S	.0759(14)	½	.4516(22)	3.4(66)
S5	S	.4036(14)	0	.1659(22)	3.3(67)
S6	S	.2639(15)	½	.1106(23)	3.1(69)
S7	S	.4341(14)	½	.3644(22)	3.7(64)
S8	(.65Se + .35S)	.0139(12)	½	.1315(19)	3.8(56)
Cu		.0529(11)	0	.4869(17)	7.15(51)

TABLE 4. Interatomic Distances and Bond Angles in Junoite*

Bond Lengths				Bond Angles			
				Bismuth		Lead	
Site							
M1	Bi(1)–S(1)	2.79(4)	x2	S(8)–Bi(1)–S(2)	86.4(1)	S(4)–Pb(1)–S(5)	83.0(1)
	S(8)	2.89(4)		S(8)–Bi(1)–S(1)	88.9(1)	S(4)–Pb(1)–S(8)	95.6(1)
	S(3)	2.95(5)		S(3)–Bi(1)–S(2)	91.4(1)	S(5)–Pb(1)–S(8)	64.3(1)
	S(2)	2.96(5)	x2	S(3)–Bi(1)–S(1)	93.2(1)	S(4)–Pb(1)–S(4)	81.0(1)
				S(2)–Bi(1)–S(2)'	86.4(1)	S(5)–Pb(1)–S(5)	78.5(1)
M2	Bi(2)–S(4)	2.50(4)		S(1)–Bi(1)–S(1)'	93.2(1)	S(8)–Pb(1)–S(8)	80.8(1)
	S(3)	2.83(4)	x2	S(1)–Bi(1)–S(2)	90.0(1)		
	S(2)	3.00(4)	x2			S(7)–Pb(1)–S(4)	69.3(1)
	S(2)'	3.33(5)				S(7)–Pb(1)–S(5)	65.0(1)
				S(2)–Bi(2)–S(2)'	97.3(1)	S(7)–Pb(1)–S(8)	128.2(1)
M3	Pb(1)–S(2)	2.94(4)		S(2)–Bi(2)–S(3)	86.4(1)	S(2)–Pb(1)–S(4)	77.4(1)
	S(4)	3.13(5)	x2	S(4)–Bi(2)–S(2)'	86.9(1)	S(2)–Pb(1)–S(8)	82.5(1)
	S(8)	3.13(5)	x2	S(4)–Bi(2)–S(3)	89.6(1)	S(2)–Pb(1)–S(5)	139.1(1)
	S(5)	3.21(5)	x2	S(2)'–Bi(2)–S(2)"	85.3(1)		
				S(3)–Bi(2)–S(3)'	91.8(1)	S(1)–Pb(2)–S(8)	88.7(1)
M4	Bi(3)–S(7)	2.65(4)	x2	S(2)–Bi(2)–S(3)	91.3(1)	S(1)–Pb(2)–S(8)'	91.4(1)
	S(5)	2.68(4)				S(8)–Pb(2)–S(8)'	90.0(1)
	S(6)	3.07(5)	x2	S(5)–Bi(3)–S(7)	83.9(1)	S(8)–Pb(2)–S(8)"	90.0(1)
	S(3)	3.50(5)	x2	S(5)–Bi(3)–S(6)	82.8(1)		
				S(7)–Bi(3)–S(7)'	99.9(1)		
				S(6)–Bi(3_–S(6)'	82.9(1)	Copper	
M5	Bi(4) S(6)	2.74(4)		S(6)–Bi(3)–S(7)	87.1(1)	S(4)–Cu(1)–S(4)'	122.2(2)
	S(5)	2.88(4)	x2			S(4)–Cu(1)–S(7)	114.3(2)
	S(6)'	2.90(4)	x2	S(3)–Bi(3)–S(7)	73.8(1)	S(4)'–Cu(1)–S(7)'	100.2(2)
	S(1)	3.07(5)		S(3)–Bi(3)–S(6)	67.8(1)	S(7)–Cu(1)–S(7)'	100.2(2)
				S(3)–Bi(3)–S(3)'	71.0(1)		
M6	Pb(2)–S(1)	2.82(4)	x2	S(3)'–Bi(3)–S(6)	113.1(1)		
	S(8)	2.87(5)	x4	S(3)'–Bi(3)–S(7)	127.6(1)		
	Cu(1)–S(4)	2.32(4)	x2	S(6)–Bi(4)–S(5)	85.4(1)		
	S(7)	2.33(5)		S(6)–Bi(4)–S(6)	88.1(1)		
	S(7)'	2.52(6)		S(1)–Bi(4)–S(5)	102.0(1)		
				S(1)–Bi(4)–S(6)	84.4(1)		
	Cu(1)–Cu(1)'	3.11		S(5)–Bi(4)–S(5)'	89.8(1)		
				S(6)–Bi(4)–S(6)'	88.1(1)		
				S(5)–Bi(4)–S(6)	90.4(1)		

* Estimated standard deviations in parentheses.

carried out with f (0.75 Se + 0.25 S) in site S(3), f (0.65 Se + 0.35 S) in site S(8), and f(S) in the other six sites. Ordering of selenium into S(3) and S(8) is further evidenced by the bond lengths of the bonds $M(1)$–S(8) = 2.89 Å and $M(2)$–S(3) = 2.83 Å, which probably would be of the order of 2.7 Å if both S(3) and S(8) were occupied by sulfur atoms. This increase in length may be explained by the larger ionic radius for selenium, 1.98 Å, as compared with 1.84 Å for sulfur (Shannon and Prewitt, 1969) and is suggested as the reason why no recognizable BiS_3 group is evident for the $M(1)$ site.

As an alternative to the above explanation, a disordered arrangement of lead and bismuth atoms, particularly in the sites $M(1)$ and $M(6)$, must also be considered. Such disordering has been discussed by Kohatsu and Wuensch (1973b) for nuffieldite (where by necessity some of the lead and bismuth atoms

must be disordered), lillianite (Takagi and Takeuchi, 1972), and hodrushite (Kupcik and Makovicky, 1968).

Bond Lengths in Bismuth Sulfosalts

Although bismuth compounds constitute about one fifth of the known sulfosalts, surveys on bond lengths in sulfides and sulfosalts (Berry, 1965; Takeuchi and Sadanaga, 1969) have only included limited data for Bi–S bonds, because reliable data were available only for galenobismutite (Iitaka and Nowacki, 1962) and cosalite (Weitz and Hellner, 1960). The aikinite structure was known (Wickman, 1935) but without distinction between the lead and bismuth positions.

It is now possible to add the data for aikinite (Kohatsu and Wuensch, 1971), nuffieldite (Kohatsu and Wuensch, 1973b), junoite, krupkaite (Mumme, 1975), hodrushite (Fig. 2a; Kupcik and Makovicky,

1968), $Cu_4Bi_4S_9$ (Fig. 2b, Ozawa and Takeuchi, 1972), wittichenite, Cu_3BiS_3 (Kocman and Nuffield, 1973, lillianite (Takagi and Takeuchi, 1972), synthetic $CuBi_5S_8$ (Ohmasa and Nowacki, 1973), and kobellite (Miehe, 1971) which has bismuth replaced by antimony to varying degrees in all metal sites. Interatomic distances for all these bismuth sulfosalts are presented in Tables 7(a) and 7(b).

Takeuchi and Sadanaga (1971) have already shown that the bond angles in TS_3 pyramids—where T is As,

TABLE 5. Comparison of Calculated and Observed Structure Factors for Junoite

h	l	y_{obs}	y_{calc}
		k = 0	
4	0	382.41	283.07
6	0	1941.34	1961.52
10	0	146.30	207.52
12	0	332.44	408.78
18	0	307.45	292.67
20	0	155.85	127.10
24	0	181.38	274.48
18	-1	367.91	422.70
16	-1	277.90	224.29
14	-1	376.20	333.83
12	-1	904.52	890.75
10	-1	477.39	405.33
8	-1	1483.56	1573.33
6	-1	717.87	682.33
4	-1	512.48	433.73
2	1	208.26	146.39
4	1	275.82	304.96
6	1	397.99	340.22
10	1	270.89	292.18
12	1	278.73	258.97
14	1	338.67	412.47
16	1	149.70	203.47
18	1	220.48	246.74
22	-2	380.67	345.89
20	-2	218.55	208.65
18	-2	326.76	363.00
16	-2	1255.11	1299.62
14	-2	1060.64	1143.18
12	-2	212.64	120.74
10	-2	1336.42	1285.83
8	-2	1527.78	1500.25
4	-2	515.52	461.77
2	-2	287.77	327.95
2	2	682.25	591.87
4	2	821.76	793.55
8	2	1104.80	1131.82
10	2	701.70	706.36
12	2	397.08	426.81
14	2	289.89	356.90
16	2	377.05	457.00
18	2	220.31	300.81
22	-3	156.19	114.43
20	-3	304.35	302.29
18	-3	142.15	202.09
14	-3	115.91	138.67
12	-3	177.90	132.71
8	-3	135.40	95.88
4	-3	710.01	695.27
0	3	360.99	298.09
2	2	546.74	591.87
6	3	1055.56	1085.86
8	3	533.59	520.55
10	3	127.23	78.02
12	3	560.86	582.77
14	3	337.37	302.05
26	-4	141.48	182.51
24	-4	343.99	364.35
22	-4	348.32	339.68
20	-4	236.48	212.17
18	-4	196.13	223.77
16	-4	218.18	287.58
12	-4	1070.70	1137.58
10	-4	178.65	109.44
8	-4	501.39	411.74
6	-4	2262.43	2160.58
2	-4	580.62	476.08
0	4	2047.26	1945.37
2	4	460.57	411.54
4	4	580.93	584.26
6	4	1125.38	1047.95
10	4	272.08	272.36
12	4	147.51	211.03
24	-5	155.43	165.59
20	-5	389.40	399.13
18	-5	304.18	343.08
16	-5	175.00	161.85
14	-5	432.47	468.34
12	-5	438.00	360.29
10	-5	551.52	539.43
8	-5	262.02	282.70
6	-5	259.00	310.29
4	-5	666.60	620.65
2	-5	381.01	248.83
0	5	499.77	435.01
2	5	195.41	129.42
4	5	908.31	936.61
8	5	187.79	174.73
10	5	288.85	299.77
12	5	405.46	482.11
18	5	266.61	321.35
22	-6	651.57	701.79
20	-6	524.04	527.88
18	-6	134.40	69.65
16	-6	796.00	866.62
14	-6	866.05	902.61
12	-6	467.47	527.36
10	-6	1046.54	1109.67
8	-6	1045.84	1048.64
6	-6	759.47	818.08
4	-6	87.24	107.01
2	-6	129.94	66.11
0	6	171.84	172.03
2	6	343.12	254.78
4	6	975.60	971.56
6	6	369.61	404.43
8	6	449.05	508.84
10	6	524.47	560.50
12	6	312.20	378.75
16	6	139.93	142.49
20	-7	204.03	253.60
18	-7	189.33	208.68
12	-7	297.55	345.12
10	-7	649.00	686.72
8	-7	467.09	466.34
6	-7	232.10	176.71
4	-7	1372.30	1274.65
0	7	365.40	275.48
2	7	1107.80	1123.74
4	7	259.71	239.70
6	7	421.50	464.60
8	7	540.43	567.13
12	7	409.17	447.41
24	-8	441.55	453.62
22	-8	152.09	205.22
20	-8	455.59	509.55
18	-8	355.87	304.15
16	-8	375.07	414.81
14	-8	285.60	303.62
12	-8	1125.76	1194.90
8	-8	462.15	400.23
6	-8	2003.11	1961.38
4	-8	356.94	259.69
2	-8	717.68	656.13
0	8	1181.74	1143.86
2	8	521.47	476.00
4	8	198.06	245.57
8	8	379.82	383.96
10	8	269.36	260.45
28	-9	203.58	202.07
26	-9	377.23	372.28
20	-9	323.69	416.16
16	-9	256.05	273.53
14	-9	695.11	767.81
12	-9	200.51	180.64
10	-9	478.25	492.15
8	-9	274.64	282.46
6	-9	441.55	432.05
4	-9	738.34	669.87
2	-9	658.54	577.64
2	9	140.70	185.44
4	9	420.95	406.71
6	9	154.72	167.13
12	9	135.34	217.27
26	-10	154.22	152.22
22	-10	699.41	810.39
20	-10	387.00	482.34
18	-10	277.97	328.86
16	-10	1023.32	1122.74
14	-10	632.46	686.07
12	-10	458.96	518.03
10	-10	401.11	346.31
6	-10	496.78	442.65
2	-10	540.77	542.86
0	10	142.39	74.78
2	10	258.85	194.40
4	10	409.37	419.47
6	10	270.21	260.67
10	10	138.15	115.66
20	-11	148.44	224.40
18	-11	403.10	478.52
16	-11	335.67	316.74
14	-11	375.59	422.87
10	-11	820.03	771.32
8	-11	321.05	259.84
6	-11	164.55	125.58
4	-11	762.31	744.09
2	-11	144.96	82.53
0	11	398.83	313.44
2	11	465.22	418.06
4	11	155.97	228.32
8	11	197.55	156.89
26	-12	306.81	291.22
24	-12	156.18	118.26
22	-12	154.75	170.00
20	-12	369.88	374.48
18	-12	414.45	481.45
16	-12	142.46	137.08
12	-12	793.45	786.40
10	-12	195.77	186.88
8	-12	243.20	180.14
6	-12	380.51	384.56
4	-12	256.57	194.42
2	-12	373.55	333.14
2	12	246.29	230.83
6	12	171.57	146.02
22	-13	155.78	74.08
20	-13	434.29	507.02
18	-13	150.57	158.18
12	-13	460.60	379.41
10	-13	358.95	301.51
8	-13	210.19	124.11
6	-13	371.06	327.42
4	-13	308.72	271.40
2	-13	270.38	190.67
0	13	190.10	151.14
4	13	278.76	208.62
28	-14	281.37	292.36
24	-14	218.98	267.28
22	-14	156.19	211.84
20	-14	155.51	236.55
18	-14	266.75	333.90
16	-14	403.72	377.86
12	-14	455.79	467.19
8	-14	308.81	274.64
4	-14	156.10	121.92
2	-14	533.54	497.39
28	-15	136.83	93.75
22	-15	155.40	108.00
20	-15	220.87	239.83
18	-15	270.22	226.22
16	-15	220.10	154.56
14	-15	466.46	415.27
12	-15	220.19	219.06
10	-15	604.49	548.71
8	-15	349.12	272.47
26	-16	317.44	327.64
20	-16	218.85	209.04
18	-16	539.05	489.53
12	-16	515.85	495.80
4	-16	198.98	167.16
28	-17	124.23	93.06
26	-17	357.70	325.36
6	-17	134.36	107.76
26	-18	178.37	154.09
24	-18	134.10	132.57
22	-18	311.75	264.85
20	-18	142.62	56.51
14	-18	246.87	241.31
12	-18	139.26	94.79
8	-18	417.16	407.18
		k = 1	
3	0	1342.57	1355.96
5	0	639.70	751.30
9	0	194.78	278.72
11	0	314.62	334.43
13	0	124.93	73.24
15	0	337.13	348.77
17	0	510.50	588.70
19	0	106.79	38.77
21	-1	149.29	175.01
19	-1	368.28	370.52
17	-1	609.00	604.65
15	-1	323.81	248.12
11	-1	1217.95	1209.72
7	-1	290.55	268.96
5	-1	1007.72	855.32
3	-1	305.38	334.22
3	1	1287.16	1286.82
5	1	845.89	787.22
7	1	128.36	54.75
11	1	312.76	347.83
13	1	263.03	327.94
19	1	211.56	191.32
21	-2	261.32	227.42
19	-2	363.38	384.75
17	-2	139.41	77.12
13	-2	509.32	504.96
11	-2	437.85	440.37
9	-2	906.18	1010.43
7	-2	702.53	608.25
3	-2	1002.15	904.18
1	-2	270.30	218.41
1	2	1016.55	881.97
3	2	1193.73	1072.55
5	2	600.52	599.28
7	2	1396.89	1379.77
9	2	159.02	121.57
11	2	397.87	408.79
13	2	793.99	880.83
21	2	182.74	217.29
25	-3	190.52	150.26
19	-3	412.23	377.47
17	-3	135.53	64.02
15	-3	213.16	163.58
13	-3	426.18	423.76
11	-3	836.41	829.59
7	-3	164.14	100.08
5	-3	901.31	801.90
3	-3	698.93	685.40
1	-3	954.46	918.58
1	3	1169.02	1124.65
3	3	219.63	288.87
5	3	1315.92	1384.37
7	3	305.35	248.21
9	3	120.98	192.38
11	3	812.81	821.39
13	3	204.16	192.78
17	3	210.71	204.96
27	-4	171.06	203.88
23	-4	335.26	336.67
21	-4	259.84	262.72
17	-4	736.57	814.67
15	-4	169.71	214.37
13	-4	456.58	458.39
11	-4	772.36	854.37
9	-4	1343.73	1373.58
7	-4	283.89	192.95
5	-4	349.92	402.37
3	-4	2192.02	2281.44
1	-4	128.64	76.88
1	4	320.90	310.39
3	4	1072.90	1049.61
5	4	363.81	438.54
9	4	290.07	325.44
11	4	488.49	595.92
15	4	452.07	540.07
19	4	125.95	78.63
27	-5	181.29	189.05
23	-5	213.33	301.02
21	-5	332.64	360.33
17	-5	746.58	817.97
15	-5	409.52	457.60
13	-5	354.11	341.43
11	-5	1507.09	1545.08
5	-5	1234.59	1206.91
3	-5	756.37	737.61
3	5	428.17	434.08
5	5	115.09	41.24
15	5	147.03	103.89
27	-6	327.20	376.43
23	-6	151.04	105.17
21	-6	208.66	169.23
19	-6	606.88	575.56
17	-6	340.55	393.96
13	-6	721.47	772.32
11	-6	483.24	540.72
9	-6	686.57	674.02
7	-6	277.19	280.77
5	-6	645.67	610.89
3	-6	780.18	705.14
1	-6	526.76	511.86
1	6	1249.79	1246.73
3	6	280.23	247.79
5	6	395.90	444.63
7	6	860.06	960.32
9	6	145.26	98.46
13	6	298.41	355.57
27	-7	363.64	298.11
25	-7	209.96	220.75
21	-7	440.03	363.86
19	-7	553.85	576.73
15	-7	290.99	234.41
13	-7	290.79	315.43
11	-7	740.39	766.60
7	-7	316.95	315.01
5	-7	1079.45	1043.35
1	-7	338.28	280.53
1	7	305.09	313.61
3	7	216.32	161.87
5	7	356.83	360.94
7	7	321.82	288.02
9	7	212.09	135.95
11	7	212.59	219.79
23	-8	301.49	278.51
21	-8	146.32	136.09
17	-8	389.20	471.01
15	-8	1013.41	1080.33
13	-8	160.80	238.31
11	-8	324.32	273.44
9	-8	1240.55	1239.72
7	-8	758.99	709.40
5	-8	106.40	137.54
3	-8	907.03	953.73
1	-8	166.54	133.00
1	8	125.95	96.24
3	8	165.16	115.14
5	8	143.28	79.73
9	8	337.20	327.25
13	8	130.94	174.16
25	-9	149.72	165.22
23	-9	336.94	426.28
21	-9	463.43	534.47
19	-9	342.10	383.95
17	-9	437.56	482.09
15	-9	215.92	142.29
13	-9	265.45	272.45
11	-9	324.27	369.88
9	-9	195.45	228.97
7	-9	196.55	126.05
5	-9	164.74	123.66
3	-9	543.78	468.79
1	-9	181.46	113.28
3	9	248.45	231.73
25	-10	259.40	250.22
23	-10	426.46	454.34
21	-10	180.43	165.08
19	-10	200.12	259.77
17	-10	270.13	366.42
11	-10	121.98	117.77
9	-10	364.21	275.58
7	-10	407.89	363.27
5	-10	566.03	509.30
1	-10	647.50	554.34
1	10	1118.34	1051.05
3	10	149.34	133.86
5	10	337.63	368.08
7	10	624.55	567.02
9	10	136.45	141.59
25	-11	149.49	155.08
23	-11	150.96	199.39
19	-11	143.93	163.99
17	-11	240.55	219.23
15	-11	134.41	124.89
13	-11	131.24	142.46
11	-11	410.32	478.46
9	-11	184.05	143.73
7	-11	529.42	473.16
5	-11	527.22	521.46
3	-11	244.11	219.10
1	-11	412.78	375.23
1	11	211.92	190.46
3	11	213.47	175.04
5	11	255.14	197.39
9	11	120.65	102.81
23	-12	261.61	281.71
21	-12	317.68	368.77
19	-12	146.62	160.28
17	-12	143.00	176.06
15	-12	1203.51	1196.84
9	-12	1276.80	1236.65
7	-12	315.08	277.62
5	-12	204.04	200.28
3	-12	661.25	583.92
1	-12	150.51	122.62
23	-13	261.04	280.33
21	-13	301.54	318.36
19	-13	149.10	92.93
17	-12	286.01	176.06
15	-13	145.07	116.56
13	-13	203.83	203.56
11	-13	204.07	158.65
9	-13	252.11	153.71
7	-13	147.57	58.94
3	-13	213.54	188.51
5	13	121.37	98.56
27	-14	136.97	131.77
23	-14	366.37	427.39
19	-14	398.85	395.17
17	-14	473.96	469.05
15	-14	149.11	103.02
13	-14	148.87	76.90
11	-14	298.53	273.01
7	-14	452.72	383.60
5	-14	452.51	418.91
1	14	424.22	399.92
3	14	169.17	176.13
27	-15	210.13	215.89
21	-15	149.81	105.23
17	-15	151.04	144.96
13	-15	213.57	193.35
11	-15	151.04	163.96
9	-15	261.06	229.55
7	-15	211.34	164.90
27	-16	127.26	91.27
25	-16	136.70	46.65
15	-16	598.74	606.17
13	-16	149.37	124.86
11	-16	209.78	184.02
5	-16	135.56	131.65
3	-16	125.59	35.19
27	-17	169.34	186.38
5	-17	118.67	82.50
25	-18	207.95	230.77
23	-18	311.31	248.53
19	-18	134.19	92.22
15	-18	134.13	30.91
9	-18	119.74	145.46
		k = 2	
26	-17	328.74	261.16
26	-16	341.85	259.69
26	-15	171.76	113.88
26	-14	220.01	143.99
26	-13	320.88	310.70
26	-12	267.28	210.43
26	-9	330.80	265.54
26	-8	266.93	192.43
26	-4	253.18	152.37
24	-14	274.57	188.65
24	-8	356.21	324.94
24	-5	139.18	118.97
24	-4	329.82	262.17
24	-3	314.40	192.35
24	-2	339.11	225.84
22	-14	203.40	157.86
22	-10	671.07	590.32
22	-6	559.87	507.62
22	-4	293.81	251.75
22	-2	311.05	244.01
22	-1	187.00	162.23
20	-16	193.78	144.03
20	-15	248.57	171.48
20	-14	208.66	163.74
20	-13	473.24	367.39
20	-12	300.76	256.01
20	-11	150.28	172.18
20	-10	366.98	341.49
20	-9	258.68	286.76
20	-8	421.71	353.34
20	-7	149.17	166.89
20	-6	472.89	374.57
20	-5	335.51	285.17
20	-4	150.40	144.22
20	-3	212.40	202.10
20	-2	210.59	155.72
20	1	188.39	159.11
18	-16	342.61	351.96
18	-15	146.04	160.94
18	-14	258.69	229.42
18	-12	367.15	330.68
18	-11	296.93	332.90
18	-10	254.15	230.36
18	-8	203.72	203.53
18	-5	251.18	245.11
18	-4	146.57	170.39
18	-3	209.73	165.77
18	-2	211.82	242.79
18	-1	368.44	301.16
18	0	259.02	212.15
18	1	253.71	187.51
18	2	281.21	205.64
18	3	262.93	244.69
16	-14	300.14	270.32
16	-11	205.94	233.43
16	-10	805.75	794.86
16	-8	237.43	272.60
16	-6	573.91	603.86
16	-4	194.93	198.43
16	-2	994.78	916.59
16	-1	207.48	155.87
16	1	212.70	140.36
16	2	365.98	323.10
14	-11	285.82	309.16
14	-10	517.31	487.19
14	-9	567.34	550.02
14	-8	129.82	183.35
14	-6	560.64	621.19
14	-5	250.45	331.53
14	-2	775.15	804.51
14	-1	274.77	223.58
14	0	284.12	262.02
14	1	358.44	282.95
14	2	365.98	243.97
14	3	300.79	214.27
12	-8	781.05	813.75
12	-6	231.32	334.43
12	-5	161.35	229.07
12	-4	626.26	770.20
12	-1	558.64	584.58
12	0	261.35	294.03
12	1	236.91	188.89
12	2	349.33	303.20
12	3	416.85	394.05
12	4	150.12	144.04
12	5	423.71	350.13
12	6	356.48	268.60
12	7	432.42	325.85
10	-6	743.17	768.13
10	-5	254.05	340.04
10	-2	821.83	885.25
10	-1	156.88	230.43
10	0	165.64	122.85
10	1	175.64	207.89
10	2	588.68	513.19
10	4	205.09	169.22
10	5	298.46	213.22
10	6	425.22	406.12
8	-4	182.39	264.79
8	-2	917.24	952.67
8	-1	911.95	980.63
8	2	749.81	757.89
8	3	440.67	348.97
8	5	142.90	134.14
8	6	363.11	365.63
8	7	475.64	399.25
8	8	296.60	284.22
6	-1	341.32	408.96
6	0	1166.96	1278.79
6	1	190.63	218.24
6	3	625.81	714.79
6	4	679.00	723.97
6	6	316.23	279.58
6	7	361.35	312.62
6	10	283.62	182.38
4	-2	125.73	297.36
4	-1	178.76	268.50
4	0	171.21	187.04
4	1	194.92	187.78
4	2	459.75	526.88
4	4	473.96	400.72
4	5	573.31	621.54
4	6	647.37	671.18
4	7	199.15	175.03
4	8	255.12	166.31
4	9	300.67	275.53
4	10	364.27	294.98
4	11	141.62	167.64
2	2	354.01	386.50
2	3	278.02	344.96
2	4	282.19	237.51
2	5	157.26	128.52
2	6	211.60	195.19
2	7	771.90	791.44
2	8	399.37	317.68
2	11	296.57	300.96
2	12	198.75	163.28
0	3	152.22	200.90
0	4	1195.09	1264.57
0	5	202.39	256.01
0	7	214.42	182.88
0	8	757.63	788.28
0	11	212.70	226.16
0	13	138.44	105.92
2	-14	427.20	365.00
2	-12	212.27	229.64
2	-10	456.92	384.34
2	-9	409.85	393.18
2	-8	439.74	465.56
2	-5	132.05	149.73
2	-4	256.86	335.25
2	-2	134.15	201.40
4	-15	451.04	363.21
4	-13	210.82	197.71
4	-12	212.46	138.29
4	-11	587.34	512.41
4	-9	415.19	471.31
4	-8	171.55	167.73
4	-7	734.66	845.00
4	-5	309.00	396.46
4	-3	338.65	440.22
4	-2	235.23	297.36
6	-16	213.77	135.00
6	-13	260.37	231.76
6	-12	298.00	271.68
6	-10	334.13	284.92
6	-9	337.17	311.19
6	-8	1235.74	1339.82
6	-6	369.02	487.67
6	-5	127.10	173.79
6	-4	1331.09	1402.32
8	-16	262.57	143.32
8	-15	285.61	187.92
8	-14	210.77	199.16
8	-11	200.40	166.94
8	-9	177.71	191.48
8	-8	234.03	274.54
8	-7	188.30	292.69
8	-6	572.72	657.01
8	-5	95.17	169.18
8	-4	223.39	264.79
10	-15	411.99	395.26
10	-13	259.62	222.36
10	-11	629.13	534.57
10	-10	231.52	254.91
10	-9	282.27	329.08
10	-7	503.22	454.23
10	-6	802.71	768.13
10	-5	293.35	340.04
12	-17	278.93	171.73
12	-16	418.70	360.95
12	-15	208.04	164.50
12	-14	368.02	329.38
12	-13	299.28	259.78
12	-12	654.06	545.78
12	-11	199.56	189.76
12	-10	427.34	345.53
12	-9	129.07	134.62
12	-8	924.15	813.75
12	-7	237.79	235.27
14	-15	330.02	301.82
14	-11	350.05	309.16
14	-10	586.57	487.19
14	-9	655.11	550.02
16	-14	335.56	270.32
16	-11	291.25	233.43

TABLE 6. Comparison of Temperature Factors for Random Se and Ordered Se

Site	Relative Fourier Peak Height	R value → 11.0%		11.9%		12.0%	
		Occupancy	Temp. Factor	Occupancy	Temp. Factor	Occupancy	Temp. Factor
S1	148	f = (S)	3.4	f = (S)	2.5	f=(.15Se+.85S)	4.1
S2	152	(S)	3.1	(S)	1.9	(.15Se+.85S)	3.4
S3	222	(.75Se+.25S)	3.0	(S)	− .3	(.15Se+.85S)	.9
S4	127	(S)	3.4	(S)	2.3	(.15Se+.85S)	3.9
S5	154	(S)	3.3	(S)	2.5	(.15Se+.85S)	4.1
S6	149	(S)	3.1	(S)	2.8	(.15Se+.85S)	4.7
S7	166	(S)	3.7	(S)	2.3	(.15Se+.85S)	4.0
S8	195	(.65Se+.35S)	3.8	(S)	1.32	(.15Se+.85S)	2.6

Sb, or Bi—approach 90° as the bond lengths between T and S progressively increase within the groups AsS_3 (98.8°), SbS_3 (94.6°), and BiS_3 (92.0°). The results in Table 7(c) give the mean angle in BiS_3 groups as 89.7°. There is however, a marked difference between the angle A and the two equal angles B in those BiS_3 groups which are joined together to form chains and in which both bridge and non-bridge bonds occur (see Fig. 3), with the mean of A greater than the mean of B by about 7°.

In these cases, as a reasonable measure of dimensions of BiS_3 groups, the following values may be proposed:

Bond length	Bridge	2.76 Å
	Non bridge	2.63 Å

Bond angle	Bridge $\wedge$ bridge	94.2° (A)
	Bridge $\wedge$ non bridge	87.5° (B)

In wittichenite (Kocman and Nuffield, 1973) the BiS_3 pyramids are isolated from each other and the three nearest sulfur atoms are closer to the bismuth atom than in any other structure. The average bond angle between these non-bridge bonds is 96.0°, and the overall coordination is close to that of a regular trigonal pyramid.

Classification of Bismuth Sulfosalts

Structural classifications for sulfides and sulfosalts have been presented by Hellner (1958), Nowacki (1969) and, more recently, Takeuchi and Sadanaga (1971).

TABLE 7a. Bismuth-Sulfur Interatomic Distances in Sulfosalts

	Shortest Distance	Second and Third	Fourth and Fifth	Others		Shortest Distance	Second and Third	Fourth and Fifth	Others
Galeno bismutite R = 10%	2.63	2.73(2)	2.99(2)	3.12	Kobellite (Bi:Sb) R = 10% 1/3,2/3	2.47	2.71(2)	2.98(2)	
	2.78	2.78,2.79	3.00,3.02(2)	3.10	5/6,1/6	2.64	2.82(2)	2.86,2.88	
Cosalite R = 25%	2.62	2.83(2)	2.85(2)	3.25	5/9,4/9	2.56	2.66(2)	2.99(2)	3.43
	2.64	2.72(2)	2.94(2)	3.25	2/3,1/3	2.54	2.77(2)	2.86(2)	3.33
	2.62	2.84(2)	3.04(2)	3.44	5/9,4/9	2.52	2.62(2)	3.03(2)	3.32
	2.54	2.66(2)	3.04(2)	3.31	1/2,1/2	2.51	2.63(2)	3.03(2)	3.53
					1/2,1/2	2.48	2.75(2)	2.88(2)	
Aikinite R = 10%	2.66	2.73(2)	2.97(2)	3.12,3.53	Junoite R = 12%	2.74	2.88(2)	2.90(2)	3.07
						2.50	2.83(2)*	3.00(2)	3.33
						2.79(2),2.89*		2.95,2.96(2)	
						2.65(2),2.68		3.07,3.50(2)	
Krupkaite R = 10%	2.65	2.79(2)	2.98(2)	3.11,3.06					
	2.54	2.79(2)	2.99(2)	3.38(2)	Lillianite R = 10%	2.64	2.82(2)	2.94(2)	3.27
	2.64	2.63(2)	2.99(2)	3.10,3.57		2.69	2.80(2)	2.98(2)	2.99
Hodrushite R = 16%	2.60	2.67(2)	3.17(2)	3.46(2)	Wittichenite R = 5%	2.57	2.60,2.61		3.43,3.558,3.71
	2.60	2.70(2)	3.12(2)	3.50(2)					
	2.55	2.71(2)	3.05(2)		CuBi₅S₈ R = 8%	2.79(2)	2.81(4)		
	2.65	2.74(2)	2.97	3.08(2)		2.59	2.83(2)	2.86(2)	
	2.73,2.67(2)		3.08(2)	3.34(2)		2.68	2.71(2)	2.94(2)	
Cu₄Bi₄S₉ R = 12%	2.75,2.67(2)		2.93,3.08(2)		Nuffieldite Pb₂Cu(PbBi)Bi₂S₇ R = 14%	2.67	2.90(2)	3.00(2)	3.33(2)
	2.60	2.83(2)	3.06(2)	3.17(2)		2.60(2)	2.62	2.99(2)	3.43
	2.57	2.68(2)	3.05(2)	3.64(2)		2.74	2.76(2)	2.93(2)	3.25,3.30
	2.65	2.73(2)	2.90(2)	3.47(2)					

* .7 Se in this Site

Hellner's classification, devised before most of the information on distortions of sulfur lattices due to the formation of TS_3 pyramids was available, was based on close packings of sulfur atoms. Nowacki discussed the configurations of anionic groups consisting of TS_3 pyramids in terms of a ϕ value, the ratio of the number of sulfur atoms to that of the T atoms in a formula unit. Nowacki then showed that possible topological features of the anionic groups are deduced for a given ϕ value.

Takeuchi and Sadanaga (1971) concentrated on the dimensional relationship between the coordination polyhedra around monovalent and divalent metal atoms (A atoms), and those around trivalent atoms (T atoms).

They concluded that the structural principle for sulfosalts of general formula $A_m T_n X_p$ (A = Ag, Cu, Pb; T = Bi, Sb, As; X = S) is the dimensional relationship between the various coordination polyhedra, and used the radii of the constituent atoms as a measure for this classification. The principal quantum number for the valence shells of the atoms was proposed to represent their atomic sizes. The average principal quantum number $\bar{n}(A)$—*i.e.*, the average size of the atoms in the unit cell—was calculated and plotted against the ratio $\dfrac{\Sigma N(A)}{\Sigma N(T)}$ which was intended to serve as an indication of the volume occupied by the A atoms relative to that occupied by the T atoms. They then constructed a diagram which indicated four distinct areas, each of which grouped together species having a common structural scheme. The bismuth sulfosalts discussed here are plotted on
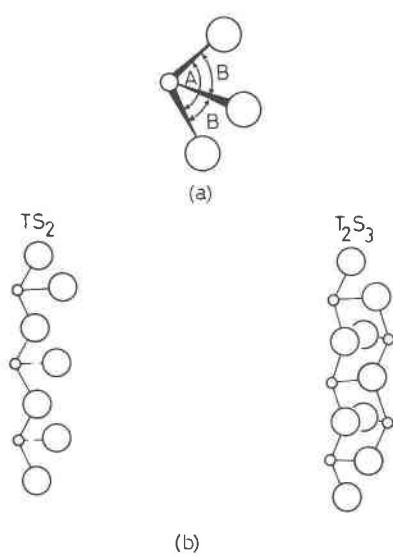
TABLE 7b. Bridge Bond and Non-Bridge Bonds on Bismuth Sulfosalts

Mineral	Bridge Bond	Non-Bridge Bond	Mineral	Bridge Bond	Non-Bridge Bond
Galenobismutite	2.79	2.63	Kobellite	2.63	2.51
	2.78			2.63	
	2.78			2.77	2.54
	2.73			2.77	
	2.73			2.78	2.48
	Av = 2.76	2.63		2.75	
				2.82	2.64
Cosalite	2.83	2.62		2.82	
	2.83			2.66	2.56
	2.74	2.64		2.66	
	2.74			2.62	2.52
	2.85	2.62		2.62	
	2.85			2.71	2.47
	2.66	2.54		2.71	
	2.66			Av = 2.91	2.53
	Av = 2.77	2.61	Junoite	2.88	2.74
Aikinite	2.73	2.66		2.88	
	2.73			2.83(.7 Se)	2.50
	Av = 2.73	2.66		2.83(.7 Se)	
Krupkaite	2.79	2.54		2.79	2.89(.7 Se)
	2.79			2.79	
	2.79	2.65		2.65	
	2.79			2.65	
	2.64			2.68	
	2.64			Av = 2.78	2.71
	2.63		Lillianite*	2.82	
	Av = 2.72	2.60		2.82	
Hodrushite	2.66	2.63		2.64	
	2.66			2.80	
	2.72	2.56		Av = 2.78	2.69
	2.72		Wittichenite		2.57
	2.73	2.51			2.60
	2.73				2.61
	2.66			Av =	2.59
	2.66		Cu Bi₅S₈	2.83	2.59
	2.76			2.83	
	2.74	2.67		2.68	
	2.75			2.71	
	Av = 2.71	2.59		2.71	
Cu₄Bi₄S₉	2.69	2.75		Av = 2.75	2.59
	2.69		Nuffieldite*	2.90	2.67
	2.83	2.60		2.90	
	2.83			2.62	
	2.68	2.57		2.60	
	2.68			2.60	
	2.72	2.65		2.76	2.74
	2.72			2.76	
	Av = 2.73	2.64		Av = 2.73	2.70

OVERALL AVERAGE Bridge Bond 2.76 Non-Bridge Bond 2.63

* Pb + Bi sites in this structure

this diagram (Fig. 4a) and fall into the expected groups with the possible exception of aikinite (PbCuBiS₃).

In this respect Takeuchi and Haga (1969) have already noted that the copper tetrahedra in seligmanite (PbCuAsS₃), the arsenic analog of aikinite, are quite regular; they describe the structure as a network of copper tetrahedra and AsS₃ pyramids, with lead occupying cavities in the framework. They therefore group seligmanite (and bournonite, PbCuSbS₃) with other copper sulfosalts into area I of Figure 4a. On the other hand Kohatsu and Wuensch (1971) show that the copper tetrahedron in aikinite is much more distorted than in seligmanite, while the PbBiS₃ chain is virtually identical with the Bi₂S₃ quadruple chain in bismuthinite. Thus seligmanite may be considered to be a copper sulfosalt, while aikinite is a true stuffed derivative of bismuthinite. Again, the PbBi₃S₆ chain in krupkaite, CuPbBi₃S₆ (Mumme, 1975) is virtually identical with those in bismuthinite and aikinite, so that krupkaite and aikinite should fall into the same group in any classification of sulfosalts.

FIG. 3. (a) The TS_3 group, showing angles A and B. (b) TS_2 and T_2S_3 chains.

TABLE 7c. Bond Angles in Bismuth Sulfosalts

Compound		Bond Angle	Average	Compound		Bond Angle	Average
Galenobismutite	Bi(1)	97.5 92.7(2)	96.3 87.1(2)	Kobellite**		93.2	93.7
	Bi(2)	95.0 81.4(2)		Junoite	M(1),Bi(1)	88.9	87.0(2)
Cosalite	M(1)	91.8 89.3(2)	94.7 90.9(2)		M(2),Bi(2)	91.8 89.6(2)	
	M(2)	98.7 93.9(2)			M(4),Bi(3)	100.0 83.9(2)	
	M(5)	91.1 91.7(2)			M(5),Bi(4)	89.8 85.4(2)	
	M(6)	99.2 88.7(2)		Lillianite**		94.3 96.5(2)	93.8 92.95(2)
Aikinite		94.9 84.2(2)	94.9 84.2(2)			93.3 89.4(2)	
Krupkaite	Bi(1)	91.6 81.2(2)	94.1 84.4(2)	Wittichenite		98.7 94.2 95.2	96.0
	Bi(2)	91.5 85.6(2)					
	Bi(3)	99.1 86.3(2)		Cu Bi$_5$S$_8$		90.5 78.9(2) 95.8 92.6(2)	93.15 85.75(2)
Hodrushite	Bi(1)	95.6 88.2(2)	93.6 86.9(2)	Nuffieldite***		88.6 86.4(2) 102.4 91.2(2)	95.1 86.9(2)
	Bi(2)	92.8 86.5(2)					
	Bi(3)	92.4 88.2(2)				94.2 83.0(2)	
	Bi(4)	95.8 85.3(2)					
	Bi(5)	91.6 86.1(2)					
Cu$_4$Bi$_4$S$_9$	Bi(1)	94.3 89.1(2)	92.7 88.5(2)				
	Bi(2)	88.7 86.9(2)					
	Bi(3)	94.7 88.7(2)					
	Bi(4)	93.0 89.3(2)					

```
  * Kobellite omitted from averages
 ** Mixed (Pb + Bi) Sites
*** The third site is octahedral
```

It is possible to reconstruct Figure 4a using

$$\frac{\Sigma N(A - \text{Pb})}{\Sigma N(T + \text{Pb})}$$

as the ordinate, as is done in Figure 4b. This has the effect of giving all lead-containing sulfosalts smaller values along the vertical scale, while leaving unaltered any sulfosalt which does not contain lead. As lead has a coordination more closely approaching that of bismuth, lead-bismuth-containing sulfosalts are thus grouped into a more recognizable category—*e.g.,* aikinite, gladite (Kohatsu and Wuensch, 1973a), and krupkaite. A disadvantage of this arrangement may be that lead-sulfosalts are concentrated at the point (0,6) on the diagram. However, following Takeuchi and Sadanaga, they can be treated separately by plotting $\frac{\Sigma N(A)}{\Sigma N(T)}$ against $\bar{n}(T)$.

Discussion

The structure of junoite is typical of lead-bismuth sulfosalts where bismuth has coordination polyhedra which simulate distorted octahedra although there are only three closest neighbors. Together with the lead octahedra, these octahedra tend to form a fragment of the galena-type structure (Hellner, 1958; Takeuchi and Sadanaga, 1969). For compounds with a high lead:bismuth ratio, distortions in the galena fragment are accommodated locally and the whole structure tends towards galena type; for intermediate values (*e.g.,* cosalite, Pb$_2$Bi$_2$S$_5$) the extent of the fragments is more limited and they join together to form a structure with intermediate polyhedra (not octahedra) in the borders of the fragments where the distortions in the structure are accumulated. In
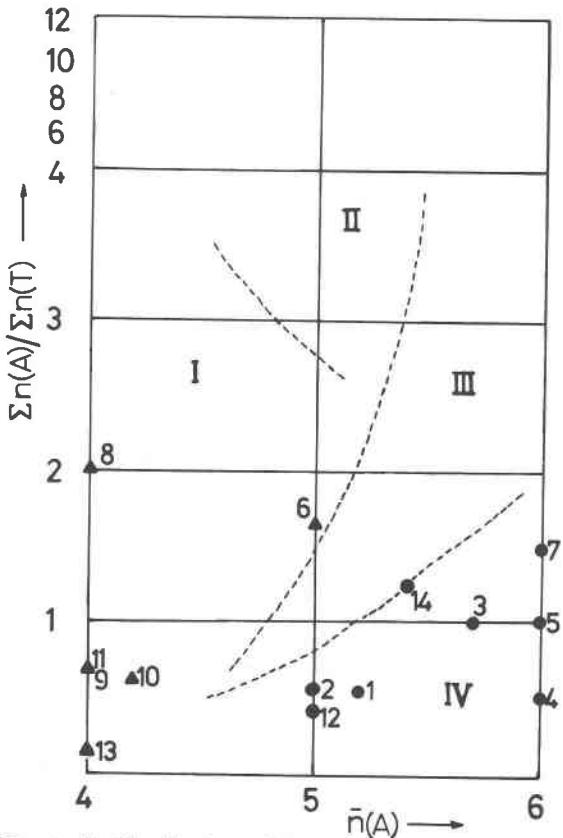
FIG. 4. (a) Classification of bismuth sulfosalts according to Takeuchi and Sadanaga, Area I (triangles): 6, aikinite; 8, wittichenite; 9, emplectite; 10, hodrushite; 11, $Cu_4Bi_4S_9$; 13, $CuBi_5S_8$. Area IV (circles): 1, junoite; 2, krupkaite; 3, kobellite; 4, galenobismutite; 5, cosalite; 7, lillianite; 12, gladite; 14, nuffieldite.

the case of junoite which has a relatively low lead:bismuth ratio (0.375), the structure consists of a grouping of intermediate polyhedra surrounded by a border of the octahedrally coordinated atoms.

Junoite samples show a range of selenium content of 3.8 to 11.6 wt percent and—as it has not been reported elsewhere either in natural occurrences of bismuth mineralization, or in synthetic studies in the Bi_2S_3–PbS–CuS system—it is unlikely that selenium-free varieties are stable. Junoite was not synthesized from $Bi_2(S,Se)_3$–$Pb(S,Se)$–$Cu_2(S,Se)$ compositions during synthetic studies carried out above 600°C (Mumme and Watts, unpublished data). Most likely selenium is an essential component of its crystal structure, ordering out during the conditions of relatively slow cooling found in the natural systems. As in the case of cosalite, which is stable only below about 425°C, experimental investigation of junoite may show that it too is a relatively low-temperature phase and of some value as an indicator of limiting thermal conditions at the time of mineralization.
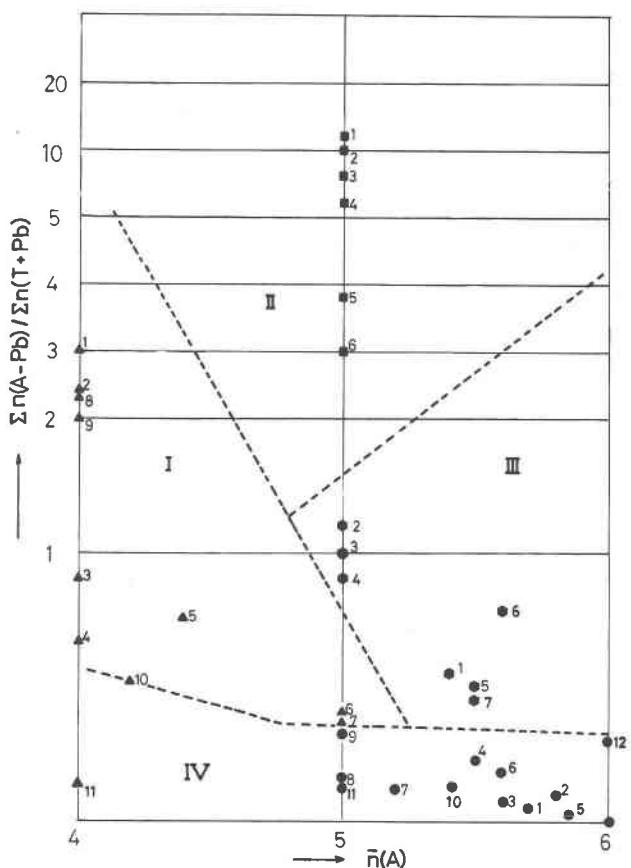
FIG. 4. (b) Classification of sulfosalts with ordinate $\frac{\Sigma N(A-Pb)}{\Sigma N(T+Pb)}$.
Area I (triangles): Cu-sulfosalts: 1, binnite; 2, tetrahedrite; 3, chalcostibnite; 4, $Cu_4Bi_4S_9$ and emplectite; 5, berthonite; 6, seligmannite; 7, bournonite; 8, nowackiite; 9, wittichenite; 10, hodrushite; 11, $CuBi_5S_8$. Area II (squares) Ag-sulfosalts: 1, polyargyrite; 2, pearceite; 3, polybasite; 4, stephanite; 5, xanthoconite; 6, pyrargyrite. Area III (hexagons) Structures based on PbS: 1, diaphorite; 2, smithite; 3, miargyrite; 4, matildite; 5, marrite; 6, hatchite; 7, freieslebenite. Area IV (circles) Lead sulfosalts: 1, kobellite; 2, fizelyite; 3, jamesonite; 4, andorite; 5, meneghenite; 6, lengenbachite; 7, junoite; 8, krupkaite; 9, aikinite; 10, nuffieldite; 11, gladite.

References

ARNDT, U. W., AND B. T. M. WILLIS (1966) *Single Crystal Diffractometry*. Cambridge University Press.

BERRY, L. G. (1965) Recent advances in sulfide mineralogy. *Am. Mineral.* **50,** 301–313.

———, AND R. M. THOMPSON (1962) X-ray powder data for ore minerals: The Peacock atlas. *Geol. Soc. Am. Mem.* **85.**

BUSING, W. R., K. O. MARTIN, AND H. A. LEVY (1962) ORFLS, a Fortran crystallographics least-squares program. *U.S. Nat. Tech. Inform. Serv.* ORNL-TM-**305.**

CROMER, D. T., AND J. T. WABER (1965) Scattering factors computed from Relativistic Dirac-Slater Wave Functions. *Acta Crystallogr.* **18,** 104–109.

CRUICKSHANK, D. W. J., D. E. PILLING, A. BUJOSA, F. M. LOVELL, AND M. R. TRUTER (1961) Computing methods and the phase problem. In, *X-Ray Crystal Analysis*. Oxford, Pergamon Press, p. 32.

DALY, J. J., F. S. STEPHENS, AND P. J. WHEATLEY (1963) *Monsanto Research, S.A., Final Report*, No. **52.**

EDWARDS, A. B. (1955) The composition of the Peko copper ore body, Tennant Creek. *Australas. Inst. Min. Metal.* **172,** 65–79.

FANDER, H. W. (1966) Selenium at Peko and Cobar. *AMDEL Bull.* (Australia), **2,** 73–75.

FLINK, G. (1910) Bidrag till Sveriges Mineralogi. *Ark. Kemi Mineral. Geol.* **3,** 4.

GRIP, E., AND A. WIRSTAM (1970) The Boliden sulphide deposit: A review of geo-investigations carried out during the lifetime of the Boliden Mine: Sweden (1924-1967). *Sver. Geol. Unders., Ser. C,* No. **651.**

HAMILTON, F. G. (1970) Operations at the Juno mine. *Reg. Meet. Austr. Inst. Min. Metal.,* Tennant Creek.

HELLNER, E. (1958) A structural scheme for sulphide minerals. *J. Geol.* **66,** 503–525.

HENDLEY, K. J., AND P. K. SCHULTZ (1972) The Bi–Pb–(Cu)–S–Se mineral in the Juno ore body, Tennant Creek. Paper presented at Spec. Meet., Geol. Soc. Austr., Canberra, February 1972.

IITAKA, Y., AND W. NOWACKI (1962) A redetermination of the crystal structure of galenobismutite. $PbBi_2S_4$. *Acta Crystallogr.* **15,** 691–698.

JOHANSSON, K. (1924a) Bedrag till Gladhammer-gruvornas mineralogi. *Ark. Kemi Mineral. Geol.* **9,** No. 8, 1–22.

—— (1924b) Ett par selenforande Mineral fran Falun Gruva. *Ark. Kemi. Mineral. Geol.* **9,** No. 8, 22–28.

KARUP-MOLLER, S. (1970) Weibullite, laitakarite, and bismuthinite from Falun, Sweden. *Geol. Foeren, Stockholm Foerh.* **92,** 181–187.

KOCMAN, V., AND E. W. NUFFIELD (1973) The crystal structure of wittichenite, Cu_3BiS_3. *Acta Crystallogr.* **B29,** 2528–2535.

KOHATSU, I., AND B. J. WUENSCH (1971) The crystal structure of aikinite $PbCuBiS_3$. *Acta Crystallogr.* **B27,** 1245–1252.

——, AND —— (1973a) The crystal structure of gladite, $PbCuBi_5S_9$ (abstr.). *Am. Mineral.* **58,** 1098.

——, AND —— (1973b) The crystal structure of nuffieldite, $Pb_2Cu(Pb,Bi)Bi_2S_7$. *Z. Kristallogr.* **138,** 343–365.

KUPCIK, V., AND E. MAKOVICKY (1968) Die Kristallstructur des Minerals $(Pb,Ag,Bi)Cu_4Bi_5S_{11}$. *Neues Jahrb. Mineral. Monatsh.* **7,** 236–237.

LARGE, R. R. (1974a) *Gold, Bismuth, Copper, Selenium Mineralization in the Tennant Creek District, Central Australia.* Ph.D. Thesis, University of New England, New South Wales.

—— (1974b) The Juno gold-bismuth-copper Mine, Tennant Creek. In, *Economic Geology of Australia and Papua, New Guinea (Metalliferous Volume).* Melbourne, Australasian Institute of Mining and Metallurgy.

——, AND W. G. MUMME (1975) Junoite, "wittite" and related seleniferous bismuth sulphosalts from Juno Mine, Northern Territory, Australia, *Econ. Geol.* **70,** 369–383.

MIEHE, G. (1971) Crystal structure of kobellite. *Nature Phys. Sci.* **231,** 133–134.

MUMME, W. G. (1975) The crystal structure of krupkaite, $CuPbBi_3S_6$, from the Juno Mine at Tennant Creek, Northern Territory, Australia. *Am. Mineral.* **60,** 300–308.

NOWACKI, W. (1969) Zur klassifikation and kristallchemie der sulphosaltze. *Schweiz. Mineral.-Petrogr. Mitt.* **49,** 109–156.

ODMAN, O. H. (1941) Geology and ores of the Boliden Deposit, Sweden. *Sver. Geol. Unders. Ser. C,* No. **438.**

OHMASA, M., AND W. NOWACKI (1973) The crystal structure of synthetic $CuBi_5S_8$. *Z. Kristallogr.* **137,** 422–432.

ONTOEV, D. O., N. V. TRONEVA, AND A. I. TSEPIN (1972) Argentiferous wittite from eastern Trans-Baikal. *Zap. Vses. Mineral. Obshch.* **101,** 476–480 (in Russian).

OZAWA, T., AND Y. TAKEUCHI (1972) The crystal structure of $Cu_4Bi_4S_9$ and its relation to simple sulphide structures. *Acta Crystallogr.* **A28,** 570.

PADERA, K. (1956) Beitrag zur Revision der mineralien aus der Gruppe von Wismutglanz und Aikinite. *Chem. Erde,* **18,** 14–18.

PEACOCK, M. A., AND L. G. BERRY (1940) Rontgenographic observations on ore minerals. *Univ. Toronto Stud. Geol. Ser.,* **44,** 47–69.

SHANNON, R. D., AND C. T. PREWITT (1969) Effective ionic radii in oxides and fluorides. *Acta Crystallogr.* **B25,** 925–946.

SINDEEVA, N. D. (1962) *Mineralogy and Types of Deposits of Selenium and Tellurium.* New York, Interscience Publ., 363 p.

TAKAGI, J., AND Y. TAKEUCHI (1972) The crystal structure of lillianite. *Acta Crystallogr.* **B28,** 349–351.

TAKEUCHI, Y., AND N. HAGA (1969) On the crystal structures of seligmannite, $PbCuAsS_3$, and related minerals. *Z. Kristallogr.* **130,** 254–260.

——, AND R. SADANAGA (1969) Structural principles and classification of sulphosalts: *Z. Kristallogr.* **130,** 346–368.

WEIBULL, M. (1885) Om selenhaltig galenobismutit fran Falun Gruva. *Geol. Foeren. Stockholm Foerh.* **96,** 657–666.

WEITZ, G., AND E. HELLNER (1960) Uber Komplex zusammengesetzte sulphidische Erze. VI. Zur Kristallstruktur des cosalits, $Pb_2Bi_2S_5$. *Z. Kristallogr.* **113,** 385–402.

WELIN, E. (1966) Notes on the mineralogy of Sweden. 5. Bismuth-bearing sulphosalt from Gladhammer, a revision. *Ark. Mineral. Geol.* **4,** 377–386.

WICKMAN, F. E. (1953) The crystal structure of aikinite, $CuPbBiS_3$. *Ark. Mineral. Geol.,* **B.1,** 501–507.

WUENSCH, B. J. (1964) The crystal structure of tetrahedrite. *Z. Kristallogr.* **119,** 437–453.